CAP37 Activation of PKC Promotes Human Corneal Epithelial Cell Chemotaxis

Gina L. Griffith,[1] Robert A. Russell,[2] Anne Kasus-Jacobi,[2,3] Elangovan Thavathiru,[1] Melva L. Gonzalez,[1] Sreemathi Logan,[4] and H. Anne Pereira[1–4]

[1]Department of Pathology, University of Oklahoma Health Sciences Center, Oklahoma City, Oklahoma
[2]Department of Pharmaceutical Sciences, University of Oklahoma Health Sciences Center, Oklahoma City, Oklahoma
[3]Oklahoma Center for Neuroscience, Oklahoma City, Oklahoma
[4]Department of Cell Biology, University of Oklahoma Health Sciences Center, Oklahoma City, Oklahoma

Correspondence: H. Anne Pereira, University of Oklahoma Health Sciences Center, Department of Pharmaceutical Sciences, 1110 N. Stonewall Avenue, CPB 329, Oklahoma City, OK 73117; anne-pereira@ouhsc.edu.

Submitted: March 18, 2013
Accepted: August 20, 2013

Citation: Griffith GL, Russel RA, Kasus-Jacobi A, et al. CAP37 activation of PKC promotes human corneal epithelial cell chemotaxis. *Invest Ophthalmol Vis Sci*. 2013;54:6712–6723. DOI:10.1167/iovs.13-12054

Purpose. The objective of this study was to elucidate the signaling pathway through which cationic antimicrobial protein of 37 kDa (CAP37) mediates human corneal epithelial cell (HCEC) chemotaxis.

Methods. Immortalized HCECs were treated with pertussis toxin (10 and 1000 ng/mL), protein kinase C (PKC) inhibitors (calphostin c, 50 nM and Ro-31-8220, 100 nM), phorbol esters (phorbol 12,13-dibutyrate, 200 nM and phorbol 12-myristate 13-acetate, 1 μM) known to deplete PKC isoforms, and siRNAs (400 nM) before a modified Boyden chamber assay was used to determine the effect of these inhibitors and siRNAs on CAP37-directed HCEC migration. PKCδ protein levels, PKCδ-Thr^{505} phosphorylation, and PKCδ kinase activity was assessed in CAP37-treated HCECs using immunohistochemistry, Western blotting, and a kinase activity assay, respectively.

Results. Chemotaxis studies revealed that treatment with pertussis toxin, PKC inhibitors, phorbol esters, and siRNAs significantly inhibited CAP37-mediated chemotaxis compared with untreated controls. CAP37 treatment increased PKCδ protein levels and led to PKCδ phosphorylation on residue Thr^{505}. Direct activation of PKCδ by CAP37 was demonstrated using a kinase activity assay.

Conclusions . These findings lead us to conclude that CAP37 is an important regulator of corneal epithelial cell migration and mediates its effects through PKCδ.

Keywords: cationic antimicrobial proteins, protein kinase C, migration, signaling, inflammation

Cellular migration or chemotaxis, a process by which cells migrate toward or away from a chemical stimulus, is required for a normal inflammatory response, resolution of infection, and wound healing.[1] During the early stages of inflammation, polymorphonuclear neutrophils (PMNs) migrate along a chemical gradient and degranulate, releasing the contents of prepackaged granules.[2] PMN granules contain important inflammatory mediators and chemoattractants that lead to the second wave of inflammation comprised mainly of a monocytic and lymphocytic infiltrate.[2] One of these mediators is a cationic antimicrobial protein of 37 kDa (CAP37), which is found within the azurophilic granules of PMNs and acts as a strong chemoattractant for monocytes.[3,4] CAP37, known initially for its antimicrobial activity, is now recognized to have a number of novel and important effects on mammalian cells.[3–6] Prior findings from our laboratory indicate that CAP37 plays a role in host defense and inflammation.[5–8] CAP37 regulates monocyte, macrophage, and microglial functions by promoting migration, phagocytosis, and activation of these cells to produce proinflammatory cytokines.[3,9,10] Furthermore, CAP37 upregulates adhesion molecules on endothelial, smooth muscle, and corneal epithelial cells.[6,8,11] Its ability to upregulate adhesion molecules and to mediate migration and proliferation of human corneal epithelial cells (HCECs) in vitro led us to postulate that CAP37 may have an important role in corneal wound healing. Its induced expression in corneal epithelial cells in response to infection suggests a role in host defense and inflammation.[5,12] The role of endogenously induced CAP37 in facilitating the healing of corneal wounds remains unknown and is the focus of future studies.

Although we have established that CAP37 regulates important host cell functions, the intracellular signaling pathways mediating these cellular processes are presently unknown. The focus of this study was to elucidate the CAP37-induced intracellular signaling mechanism that promotes migration, an essential step in wound healing, using the corneal epithelial cell in an in vitro model of chemotaxis. Since previous studies have shown that CAP37 activates the protein kinase C (PKC) pathway in rat endothelial cells,[13] we hypothesized that the PKC signaling pathway may be involved in CAP37-facilitated HCEC migration.

PKC belongs to a multigene, serine/threonine like family of kinases. The PKC pathway is activated through G protein–coupled receptors (GPCRs) and other growth factor receptors that activate phospholipases.[14–16] Phospholipases hydrolyze phospholipids into diacylglycerol (DAG), which activates PKC. Activation of the PKC pathway has been shown to regulate

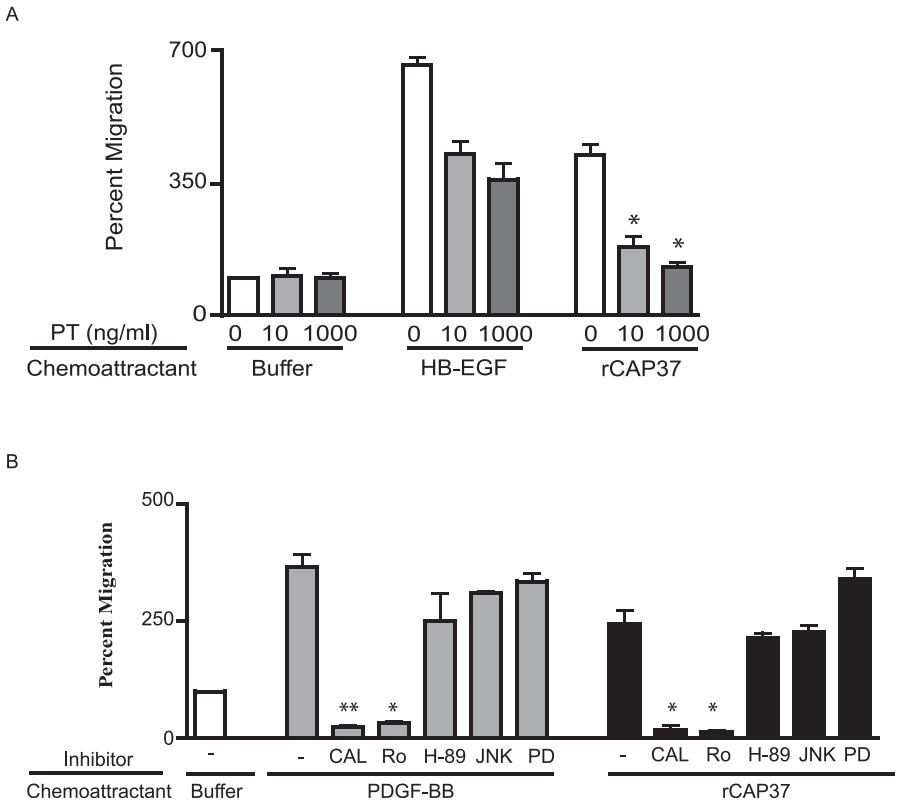

Figure 1. Chemotaxis of HCECs in response to CAP37 is mediated by PKC signaling through a G protein-coupled receptor. (**A**) Effect of PT (0, 10, 1000 ng/mL) treatment on HCEC chemotaxis in response to the buffer control (0.1% BSA in Gey's buffer), HB-EGF (50 ng/mL), or rCAP37 (250 ng/mL) as determined by the modified Boyden chemotaxis chamber method. HCECs were treated with PT for 2 hours at 37°C and chemotaxis measured in response to HB-EGF and rCAP37 after incubation for 3 hours at 37°C. Chemotaxis is expressed as a percent of the buffer control (no chemoattractant) that is arbitrarily assigned the value of 100% migration. Data are expressed as mean ± SEM and are calculated from six observations for each test point. $^{*}P < 0.05$ by Wilcoxon signed-rank test as compared with controls not treated with PT. (**B**) Effect of pharmacological inhibitors on HCEC chemotaxis. HCECs were treated with PKC inhibitors calphostin c (50 nM, CAL) and Ro-31-8220 (100 nM, Ro); PKA inhibitor H-89 (48 nM); JNK inhibitor II (40 nM); or MAPK inhibitor PD98059 (50 μM) for 1 hour at 37°C. HCEC chemotaxis was measured in response to the buffer control (0.1% BSA in Gey's buffer); PDGF-BB (20 ng/mL); or rCAP37 (250 ng/mL) by the modified Boyden chemotaxis chamber method. Chemotaxis is expressed as a percent of the buffer control (no chemoattractant) that is arbitrarily assigned the value of 100% migration. Data are expressed as mean ± SEM calculated using three observations for each test point. $^{**}P < 0.01$, $^{*}P < 0.05$ by Dunn's multiple comparison test as compared with controls not treated with inhibitors.

cellular processes including migration, proliferation, differentiation, and gene expression in a number of different cell types.[16] The 11 known isoforms of PKC are divided into three subfamilies: classical, novel, and atypical. Classical PKCs require the presence of both DAG and calcium for maximal activation. Novel PKCs require only DAG for activation and atypical PKCs are activated by interactions with phospholipids on the plasma membrane. PKCs regulate cellular function by phosphorylation of serine/threonine residues on substrate proteins.[17,18]

To establish the intracellular signaling pathway involved in CAP37-facilitated HCEC migration, we used a number of different technical approaches that included pharmacological inhibitors, siRNA, immunodetection, and a kinase activity assay. Our data demonstrate that CAP37 mediates HCEC migration through the activation of a GPCR and activates the PKC signaling pathway, specifically the PKC isoform δ. This study establishes the mechanism through which CAP37 induces migration in HCECs and thereby provides a potential means to identify therapeutic targets to modulate the corneal inflammatory response that could promote wound healing. To our knowledge, this is the first study that identifies the signaling pathway responsible for the process of chemotaxis of human corneal epithelial cells in response to a neutrophil-derived cationic antimicrobial protein.

Methods

Antibodies

Mouse primary antibodies anti-PKC α, β, γ, ε, θ, ι, and λ were from Becton Dickinson (Bedford, MA) and anti-PKCδ, η, and ζ were from Santa Cruz Biotechnology, Inc. (Santa Cruz, CA). Rabbit antiphosphorylated PKCδ-Thr^{505} and mouse anti β-actin were obtained from Sigma-Aldrich (St. Louis, MO). For Western blotting, secondary horseradish peroxidase rabbit and mouse antibodies were purchased from Cell Signaling Technology (Danvers, MA) and Jackson ImmunoResearch (West Grove, PA), respectively. Secondary AlexaFluor 488 goat anti-mouse antibody was purchased from Molecular Probes (Eugene, OR). A monospecific, rabbit antiserum shown to be specific for CAP37 has been previously described.[13]

Cell Culture

SV-40 adenovirus immortalized HCECs were a gift from James Chodosh (Boston, MA) and were maintained as previously described[5,19] in defined keratinocyte-serum free media (keratinocyte serum-free media [SFM]; Gibco, Grand Island, NY) containing L-glutamine (2 mM; Gibco); antibiotic-antimycotic (0.1 units/mL penicillin G sodium, 100 μg/mL streptomycin sulfate, 0.25 μg/mL amphotericin B; Gibco); and growth

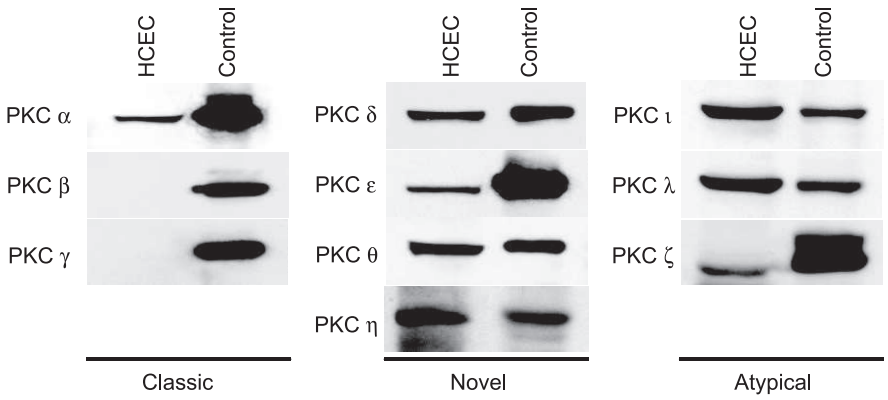

Figure 2. Constitutive expression of classical (α, β, γ); novel (δ, ε, θ, η); and atypical (ι, λ, ζ) PKC isoforms in HCECs. Western blot analysis of 100 μg protein from HCEC lysates and 15 μg protein from rat cerebrum lysate (used as positive control for PKC isoforms α, β, γ, δ, ε, η, ζ, ι, and λ), or 15 μg protein from control Jurkat cell lysate (used as positive control for PKCθ). Primary antibodies for PKC isoforms were used as described in the Methods section.

supplements as provided by the manufacturer. HCECs were used between passages 10 and 20.

Primary human corneal epithelial cells were cultured from donor corneas procured through the Lions Eye Bank (Oklahoma City, OK). Quadrisected corneas were incubated overnight at 4°C on ice in Hank's balanced salt solution (Gibco) containing dispase (25 caseinolytic U/mL; Becton Dickinson) and 5 μg/mL gentamicin (A.G. Scientific, Inc., San Diego, CA).[20] Corneal epithelial cells were then detached from the stroma by gently scraping the corneal surface with a scalpel. The removed cells were digested for 5 minutes in 0.25% trypsin-EDTA (Gibco) at 37°C followed by the addition of an equal volume of heat inactivated fetal bovine serum (FBS; Gibco) and were centrifuged at 450*g* for 5 minutes. The cell pellet was resuspended in keratinocyte-SFM containing growth supplements and the cells were seeded onto a tissue culture dish treated with commercial coating mix consisting of fibronectin, collagen, and albumin (FNC Coating Mix; AthenaES, Baltimore, MD). All HCECs were starved for 18 hours in keratinocyte-SFM without growth factors prior to the performance of experiments.

Production of Recombinant CAP37

Recombinant CAP37 (rCAP37) was produced as described previously using an RSV-PL4 expression vector in human embryonic kidney 293 cells, and purified on an HPC4 immunoaffinity column.[6,21,22] All batches of rCAP37 were dialyzed in 0.01% acetic acid and characterized for purity by SDS-PAGE and Western blot analysis and routinely screened for biological activity using the modified Boyden chemotaxis chamber assay as formerly published.[3,23] All functionally active rCAP37 used in this study was tested for endotoxin levels as determined by the limulus amebocyte lysate assay (QCL 1000; Lonza, Basel, Switzerland) and contained less than <0.05 endotoxin units per microgram of protein.

Pharmacological Inhibitor Studies

To determine if CAP37-induced signaling occurred through a GPCR, HCECs were treated with 10 or 1000 ng/mL of pertussis toxin (PT; Sigma-Aldrich) for 2 hours at 37°C before being harvested for chemotaxis. To determine which of the common signaling pathways mediated CAP37-induced chemotaxis, a number of pharmacological inhibitors were employed. HCECs were treated with the PKC inhibitors calphostin c (50 nM; Calbiochem, Gibbstown, NJ), and Ro-31-8220 (100 nM; Calbiochem), the protein kinase A (PKA) inhibitor H-89 (48 nM; Calbiochem), the c-Jun N-terminal kinase (JNK inhibitor II, 40 nM; Calbiochem), and the mitogen-activated extracellular-signal-regulated kinase (MEK) inhibitor PD 98059 (50 μM; Calbiochem). HCECs were treated with each of these inhibitors for 60 minutes at 37°C before being harvested for chemotaxis. PKC depletion was achieved by treating HCECs with 200 nM of phorbol 12, 13-dibutyrate (PDBu; Sigma-Aldrich) or primary HCECs with 1 μM phorbol 12-myristate 13-acetate (PMA; Sigma-Aldrich) for 20 hours before the chemotaxis assay was performed.[16]

Chemotaxis

Chemotaxis assays were performed using the modified Boyden chemotaxis chamber assay described previously.[3,23] HCECs were cultured as described above until they reached 70% confluency. Cells were split to less than 70% confluency and cultured in keratinocyte-SFM without growth factors overnight the day before experimentation. Cells were detached using 5 mM EDTA in PBS at 37°C for 30 minutes. Trypan blue staining was used to distinguish between dead and living cells in cell counts. Only live cells were counted ensuring that 8×10^5 living cells/mL were used per experiment. Cells were adjusted to a concentration of 8×10^5 cells/mL in Gey's buffer (Sigma-Aldrich) containing 0.1% endotoxin-low BSA (Sigma-Aldrich). rCAP37 was used at concentrations of 250 and 500 ng/mL. Controls included heparin binding–epidermal growth factor (HB-EGF, 50 ng/mL; R&D Systems, Minneapolis, MN), platelet-derived growth factor-BB (PDGF-BB, 20 ng/mL; R&D Systems), and Gey's buffer containing 0.1% endotoxin-low BSA (negative control; Sigma-Aldrich). Chambers were set up in triplicate for each experimental condition. After 3 hours incubation at 37°C, filters were stained and chemotaxis was determined by counting the number of cells that had migrated to the underside of each filter. Ten adjacent fields were counted per filter under a ×40 objective and averaged. Chemotaxis was expressed as percent migration compared with the Gey's buffer control, which was arbitrarily defined as 100% migration.

Protein Extraction and Western Blot Analysis

Cell lysates were prepared by removing HCECs from tissue culture dishes with a cell scraper. The cells were washed twice with ice-cold PBS (Gibco). Cells were lysed in Kinexus lysis buffer (Vancouver, British Columbia, Canada; 20 mM morpho-

Investigative Ophthalmology & Visual Science

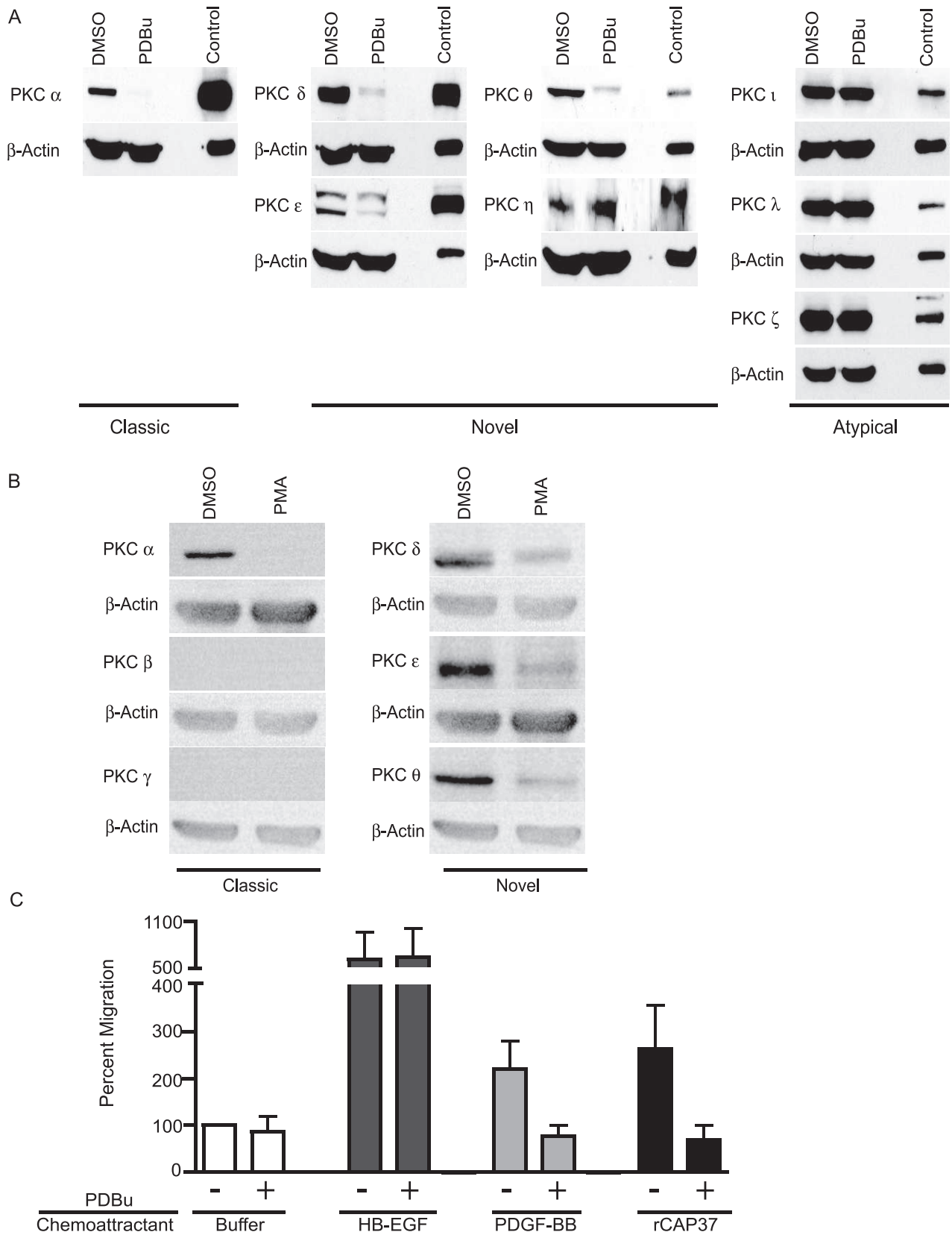

Figure 3. CAP37-mediated HCEC chemotaxis occurs through a classical or novel PKC isoform. (**A**) HCECs were treated with 200 nM PDBu dissolved in DMSO or an equal volume of DMSO (vehicle control) in basal media for 20 hours at 37°C. Western blot analysis was performed on 50 μg protein from vehicle-treated HCEC lysates (DMSO), PDBu-treated HCEC lysates (PDBu), and 15 μg rat cerebrum lysates or Jurkat cell lysates (control) using primary antibodies described in the Methods section. β-actin levels were determined for each blot. (**B**) Effect of 20 hours PMA (1 μM) treatment on PKC isoform expression on primary HCECs. Western blot analysis was performed on 30 μg protein from vehicle-treated (DMSO) and PMA-treated (PMA) primary HCEC lysates. Blots were probed for PKC isoforms δ, ε, and θ and stripped and probed for β-actin. The blots were then

Investigative Ophthalmology & Visual Science

probed for PKC isoforms β, α, and γ, respectively. The corresponding β-actin controls are shown for each blot. (**C**) Effect of PKC depletion following PDBu treatment on HCEC migration. HCECs were treated for 20 hours with PDBu (200 nM) and chemotaxis in response to the buffer control (0.1% BSA in Gey's buffer); PDGF-BB (20 ng/mL); HB-EGF (50 ng/mL); or rCAP37 (250 ng/mL) was determined by the modified Boyden chemotaxis chamber method. Chemotaxis results are expressed as a percent of the buffer control (no chemoattractant) that is arbitrarily assigned the value of 100% migration. Data are expressed as mean ± SEM calculated using three observations for each test point.

linepropanesulfonic acid minimal media, pH 7.0); 2 mM ethylene glycol tetraacetic acid); 5 mM EDTA; 30 mM sodium fluoride (NaF); 40 mM β-glycerophosphate, pH 7.2; 10 mM sodium pyrophosphate; 2 mM sodium orthovanadate; 3 mM benzamidine; and 0.5% Triton X-100; final pH adjusted to 7.0); or radioimmunoprecipitation assay buffer (Cell Signaling Technology). Lysis buffers were supplemented with 5 μM pepstatin A (Sigma-Aldrich); 10 μM leupeptin (Sigma-Aldrich); and 1 mM phenylmethylsulfonyl fluoride (PMSF; Sigma-Aldrich). Cells were sonicated (3 pulses at 10 seconds per pulse at 35%) using a sonic dismembrator (Fisher Sonic Dismembrator Model 300; Thermo Fisher Scientific, Inc., Pittsburgh, PA) and lysates were centrifuged at 16,000*g* for 10 minutes. Protein concentrations in supernatants were determined using the bicinchoninic acid protein concentration assay (Pierce Chemical Co., Rockford, IL).

Equal amounts of each lysate, based on protein concentration, were loaded and analyzed by SDS-PAGE followed by transfer to nitrocellulose membranes (Whatman, Inc., Florham Park, NJ) for Western blot analysis.[24] Nitrocellulose membranes (Whatman, Inc.) were incubated at 4°C overnight with primary antibodies at concentrations specified by the manufacturer. Rat cerebrum or Jurkat cell lysates were used as positive controls for PKC isoform expression. Blots were washed and incubated for 1 hour at room temperature with rabbit or mouse secondary antibody conjugated to horseradish peroxidase. Secondary antibodies were used as specified by the manufacturer. Blots were developed using a Western blotting substrate (Pierce ECL Western Blotting Substrate; Thermo Fisher Scientific Inc.) and analyzed using a commercial imaging system (UltraLum Imager; Omega, Claremont, CA).

siRNA Transfection and Gene Silencing in HCECs

For transfection with siRNAs, cells were cultured to 50% to 70% confluence, detached using a cell dissociation reagent (TrypLE Express; Gibco) and centrifuged at 450*g* for 5 minutes. The cell pellet was washed twice in PBS. The pellet was resuspended in cold keratinocyte-SFM (Gibco) without growth supplements. siRNA (400 nM of PKC δ, ε, θ, or scrambled siRNA-A; Becton Dickinson) was added to the cell suspension (5.0×10^5 cells) and incubated for 10 minutes on ice prior to electroporation (230 volts, 500 farads, ∞ ohms) using a commercial electroporation system (Gene Pulser Xcell Total System; Bio-Rad Lab, Inc., Los Angeles, CA). Following electroporation, cells were seeded and cultured as previously stated. The efficiency of each knockdown was confirmed 72 hours posttransfection by Western blot analysis of cell lysates. Preliminary studies to optimize knockdown efficiency indicated that maximum knockdown was achieved at 72 hours posttransfection at the stated dose.

Immunocytochemistry and Confocal Microscopy

HCECs were grown on glass chamber slides (LabTek II; Nalge Nunc International, Rochester, NY). Cells were treated with rCAP37 (500 ng/mL), PDGF-BB (20 ng/mL), 1 μM PMA (positive control), or 0.01% acetic acid (Thermo Fisher Scientific Inc., negative control). Following treatment, cells were fixed in 4% (vol/vol) formaldehyde (Thermo Fisher Scientific Inc.) in PBS for 20 minutes at room temperature followed by permeabilization in 0.5% Triton X-100 (Mallinckrodt, St. Louis, MO) in PBS for 10 minutes. All remaining formaldehyde was quenched with 0.05 M NH_4Cl (Sigma-Aldrich) in PBS for 10 minutes. Cells were washed in PBS and incubated in blocking buffer (10% [vol/vol], normal donkey serum in PBS containing 5% BSA, and 0.5% Triton X-100) for 1 hour at room temperature. Cells were incubated for 1 hour at room temperature in mouse anti-PKCδ (500 ng/mL); mouse anti-PKCθ (1 μg/mL); or mouse IgG control (1 μg/mL; Jackson ImmunoResearch). After washing in PBS containing 0.25% Triton X-100, the cells were incubated in secondary antibody (4 μg/mL in blocking buffer; AlexaFluor 488 goat anti-mouse) for 1 hour at room temperature. Cells were washed three times for 5 minutes in PBS followed by a final wash in water before mounting in commercial mounting medium containing DAPI (Prolong Gold Anti-fade; Molecular Probes, Eugene, OR). Confocal images were obtained using an inverted microscope (Leica TNS NT Confocal; Nikon, Melville, NY). Images shown were compiled from 15 sections of 0.5 to 1.5 μm separation and represent the entire *z*-axis of the cells. Image analysis was performed using commercial software (Leica LCS Lite; Leica Microsystems, Wetzlar, Germany).

Kinase Activity Assay

HCECs were starved for 2 hours prior to being treated with rCAP37 (250 ng/mL) or 0.01% acetic acid (negative control) for 5 or 15 minutes. Cells were manually removed from each tissue culture dish using a cell scraper. Cell lysates were made in ice-cold PBS containing 5 μM pepstatin, 10 μM leupeptin, and 1 mM PMSF using a commercial mixer (Polytron PT 1200 CL; Kinematica AG, Luzern, Switzerland) for 1 minute at max speed. Lysates were centrifuged at 16,000*g* for 10 minutes and the pellet discarded. Protein levels of each sample were adjusted to the same concentration. Lysates were incubated with anti-PKCδ (1–2 μg per 100–500 μg protein) overnight at 4°C followed by 3 hours incubation with a commercial reagent (Protein G PLUS-Agarose beads, 20 μL per immunoprecipitation reaction; Santa Cruz Biotechnology Inc.) at 4°C. Lysates were centrifuged at 1000*g* for 3 minutes. Supernatant was removed and the beads were washed three times in ×1 kinase reaction buffer (40 mM Tris-HCl, 20 mM $MgCl_2$, 0.1 mg/mL BSA, pH 7.5). Beads were resuspended in kinase reaction buffer in preparation for the kinase activity assay. Equal amounts of beads from the immunoprecipitation reaction were incubated with ATP (50 μM; Promega, Madison, WI) and a commercial substrate (CREBtide, 0, 1, or 2 μg; SignalChem, Richmond, BC, Canada) for 1 hour at room temperature. Kinase activity was determined using a kinase assay (ADP-Glo; Promega) as specified by the manufacturer's instructions. Luminescence was determined using a luminometer (Synergy 2; Bio Tek Instruments, Inc., Winooski, VT). Samples were run in triplicate.

Statistical Analysis

Chemotaxis experiments were analyzed using a Kruskal-Wallis test followed by Dunn's multiple comparison test post hoc or a Wilcoxon signed-rank test. Phosphorylation studies were analyzed using an unpaired *t*-test. A Wilcoxon signed-rank test was used to analyze kinase activity data. Statistics were calculated using commercial software (GraphPad Prism 4.03; GraphPad Software, Inc., San Diego, CA). The mean of

Investigative Ophthalmology & Visual Science

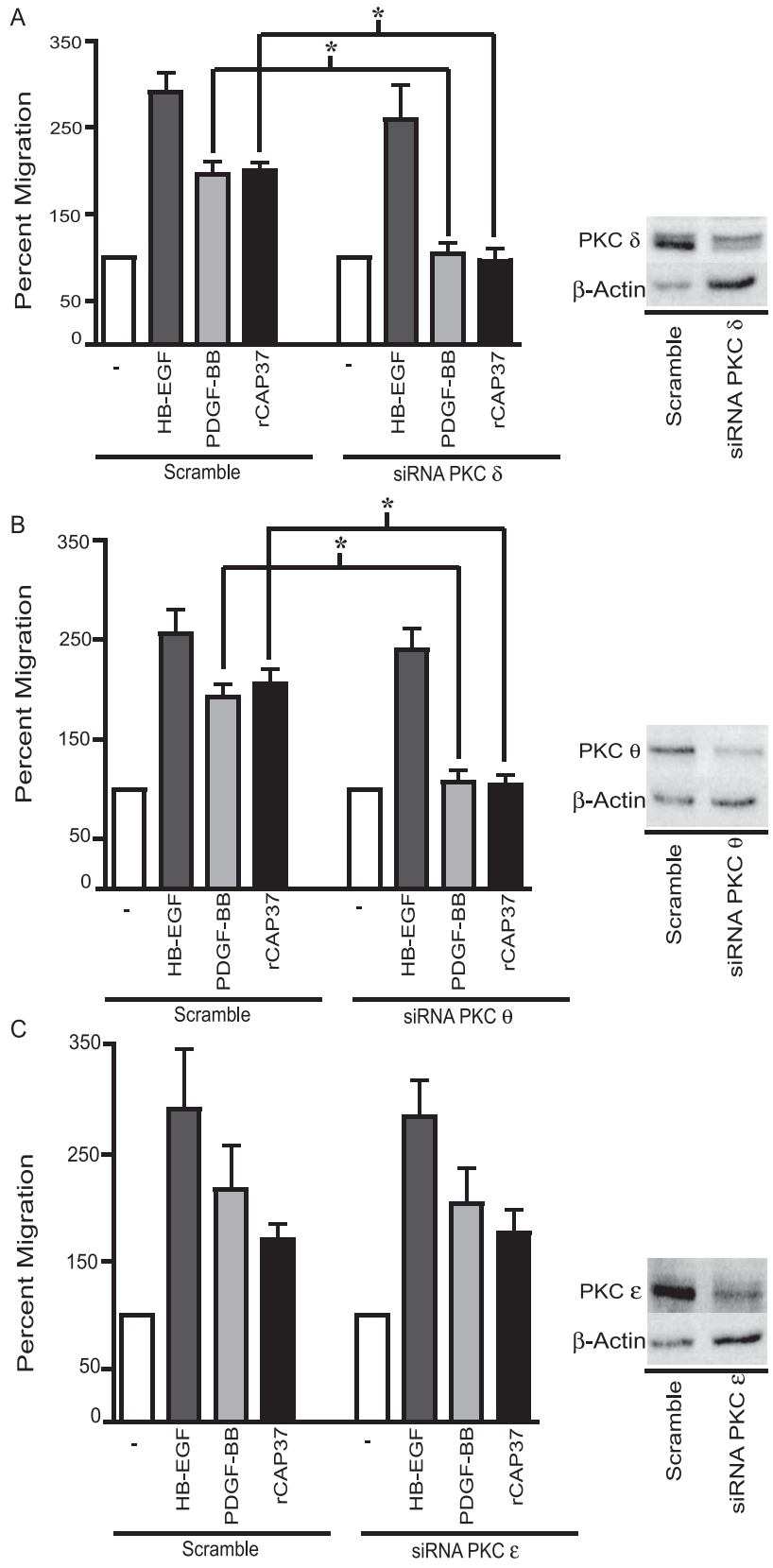

Figure 4. PKCδ and PKCθ isoforms are required for CAP37-mediated chemotaxis of HCECs. HCEC chemotaxis performed with cells that were transfected with siRNAs directed against (**A**) PKCδ, (**B**) PKCθ, or (**C**) PKCε, and scrambled siRNA. HCECs were transfected as described in the Methods section and chemotaxis in response to HB-EGF (50 ng/mL); PDGF-BB (20 ng/mL); or rCAP37 (500 ng/mL) was determined 72 hours after transfection using the modified Boyden chamber chemotaxis assay. Chemotaxis results are expressed as a percent of the buffer control (no chemoattractant) that is arbitrarily assigned the value of 100% migration. Data are expressed as mean ± SEM and are representative of four independent experiments performed in triplicate. *$P < 0.05$ by Wilcoxon signed-rank test as compared with controls transfected with scrambled

Investigative Ophthalmology & Visual Science

siRNA. Knockdown efficiency for each experiment was determined by Western blot analysis of 40 μg protein from HCEC lysates. Samples were analyzed using anti-PKCδ, PKCθ, and PKCε antibodies. Representative blots including the β-actin loading controls are shown.

independent experimental values are shown ± SEM and a P value < 0.05 was considered significant for all statistical analyses.

Results

CAP37 Activates PKC Through a GPCR

To elucidate the signaling pathways through which CAP37 mediates HCEC migration, HCECs were treated with PT, a well-characterized disruptor of GPCR signaling[25,26] and migration in response to CAP37 (250 ng/mL) was measured using the modified Boyden chemotaxis chamber assay. Treatment with 10 and 1000 ng/mL PT was found to significantly inhibit CAP37-mediated migration of HCECs (Fig. 1A). Migration decreased to basal levels following treatment with 1000 ng/mL PT. Migration in response to HB-EGF, a ligand for tyrosine-kinase receptor, used as a control in these experiments indicated no significant ($P = 0.0625$) reduction in chemotaxis following PT treatment, as expected.[27–29] Previous studies on EGF signaling in human embryonic kidney cells (HEK 293) indicated that, even though the HB-EGF receptor is not a GPCR, PT partially affects EGF-mediated chemotaxis,[30] which likely explains the partial reduction in chemotaxis seen in our assays as well.

CAP37 has been shown to share sequence homology with human neutrophil elastase (44%) and cathepsin G (32%), two other azurophilic granule proteins. Elastase and cathepsin G have been shown to act as GPCR agonists[31,32] and, as a result, we hypothesized that CAP37 might also signal through a GPCR. Since it is known that GPCRs can activate intracellular pathways,[33,34] experiments were carried out to investigate which signaling pathway(s) is activated by CAP37 to regulate migration. PDGF-BB, a well-characterized growth factor known to mediate chemotaxis through PKC,[35] was used as a control. Treatment with the PKC inhibitors calphostin c and Ro-31-8220 significantly attenuated CAP37 and PDGF-BB mediated chemotaxis. PKA inhibitor H-89 and mitogen-activated protein kinase (MAPK) inhibitors (JNK inhibitor II and PD 98059) did not significantly reduce cell migration in response to CAP37 or PDGF-BB (Fig. 1B). These results suggest the participation of PKC in CAP37-mediated migration.

All PKC Isoforms Are Expressed Constitutively in HCEC Except PKC β and γ

We first sought to determine which of the 11 PKC isoforms could be involved in CAP37-mediated migration. Western blot analysis of HCEC protein extracts demonstrated the constitutive expression of the classical isoform α, the novel isoforms δ, ε, θ , and η, and the atypical isoforms ι, λ, and ζ in these cells. The two classical isoforms β and γ were not detected in HCEC in contrast to their detection in positive control lysates (Fig. 2).

Treatment With Phorbol Esters Inhibits CAP37-Mediated HCEC Migration

Extended treatment with a phorbol ester (PDBu or PMA) was used to selectively deplete the classical and novel PKC isoforms.[36] Immunoblotting confirmed depletion of the classical PKC isoform α, and novel PKC isoforms δ, ε, and θ (Fig. 3A). PDBu treatment did not deplete the novel PKCη isoform and atypical PKCs (Fig. 3A). Primary HCECs treated with PMA showed similar constitutive expression and depletion of PKC α, δ, ε, and θ isoforms (Fig. 3B).

The modified Boyden chamber chemotaxis assay was used to quantify the inhibition of CAP37-mediated HCEC migration following PDBu treatment. PDGF-BB and HB-EGF were used as controls. CAP37- and PDGF-BB-dependent migration was fully inhibited after PDBu treatment (Fig. 3C), whereas HB-EGF migration was unaffected. These results suggest that PKC isoforms α, δ, ε, and/or θ mediate CAP37-induced HCEC chemotaxis.

CAP37 Mediates HCEC Migration Through PKC δ and θ

To further elucidate and validate the involvement of PKC isoforms in CAP37-dependent HCEC migration, HCECs were treated with specific siRNAs directed against PKC δ, θ, ε, or α. PDGF-BB and HB-EGF were used as positive controls. HCECs transfected with siRNA directed against PKC isoforms δ (Fig. 4A) and θ (Fig. 4B) showed a complete inhibition of migration in response to chemoattractants CAP37 and PDGF-BB (Figs. 4A, 4B). By contrast, there was no significant change in migration in response to HB-EGF after siRNA treatment (Figs. 4A, 4B). In HCECs transfected with siRNA directed against PKCε (Fig. 4C) and α (data not shown), there was no significant inhibition of HB-EGF, PDGF-BB, and CAP37 induced migration when compared with HCECs transfected with a scrambled siRNA control. The efficiency and specificity of each knockdown was confirmed by immunoblot analysis. Representative Western blots are shown in Figures 4A, 4B, and 4C. These results suggest the requirement for PKCδ and PKCθ, but not PKCε and PKCα for CAP37-mediated HCEC migration.

CAP37 Increases PKCδ Expression in HCECs

Experiments were conducted to determine PKCδ and PKCθ expression levels following CAP37 treatment. Confocal studies revealed an increase in PKCδ (Fig. 5A) staining in response to 250 and 500 ng/mL CAP37 at 5 and 15 minutes. A slight increase in PKCθ staining (Fig. 5A, right panel) was also seen at 15 minutes in CAP37-treated cells. The strongest staining of PKCδ and PKCθ was seen at 15 minutes with 500 ng/mL treatment of CAP37. However, the staining for PKCδ was considerably stronger than PKCθ. An increase in staining for PKCδ and PKCθ was also seen in PMA-treated (positive control) cells. No staining was seen when a mouse IgG was used in place of these primary antibodies (data not shown). To confirm that the increase in PKCδ and PKCθ staining was a specific effect of CAP37 treatment, HCECs were treated with CAP37 that had been immunoadsorbed with an anti-CAP37 antibody (Fig. 5B). Results show an increase in staining for PKCδ and PKCθ in PDGF-BB–treated (positive control) samples regardless of treatment with anti-CAP37. In cells treated with immunoadsorbed CAP37, the amount of staining for PKCδ and PKCθ was comparable with basal levels. Since the levels of staining for PKCδ were stronger than those obtained with PKCθ, we selected to focus on PKCδ in this study.

PKCδ Phosphorylation and Kinase Activity in CAP37-Treated HCECs

The amount of PKCδ protein, its level of phosphorylation, and kinase activity were further studied.

Investigative Ophthalmology & Visual Science

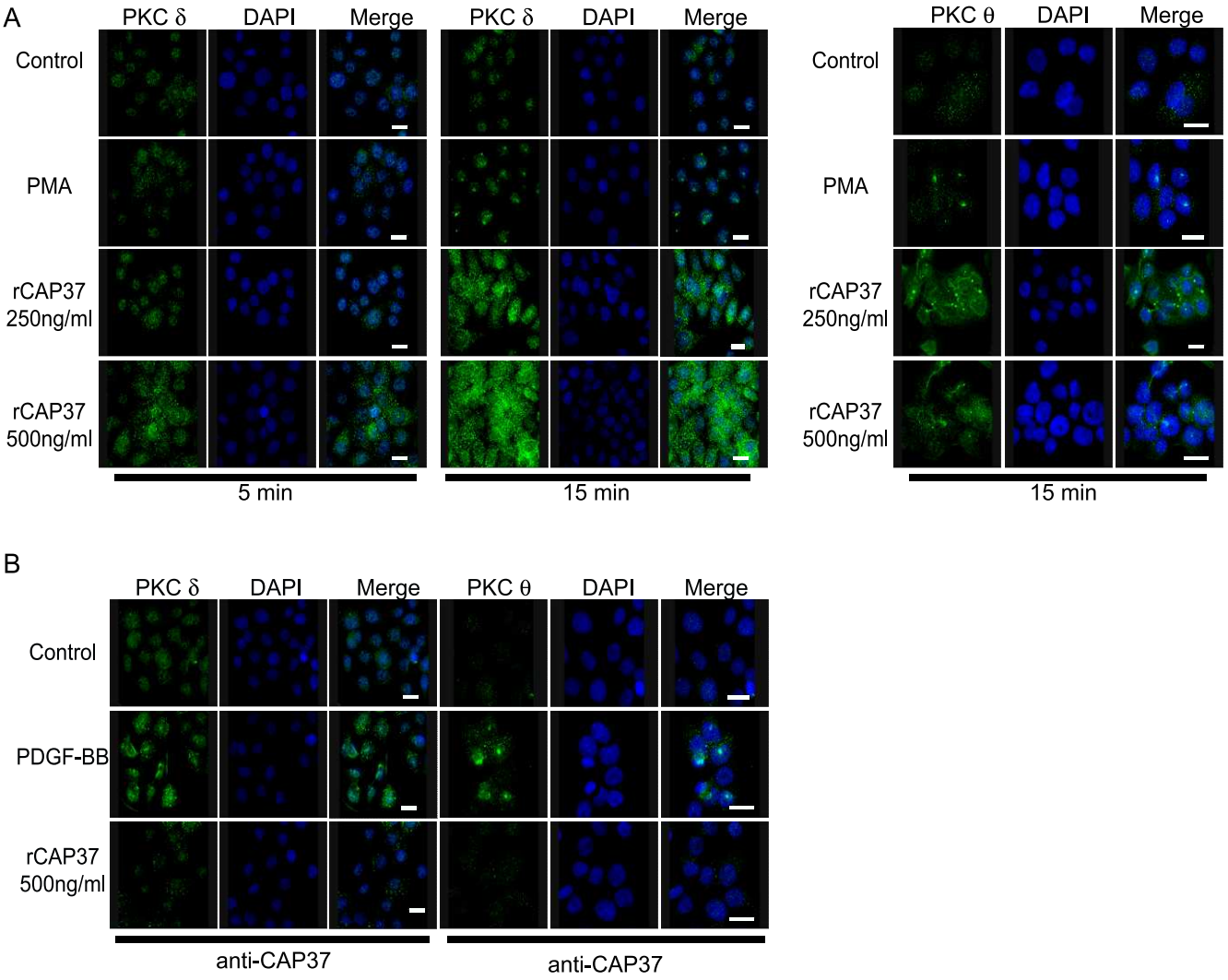

Figure 5. CAP37 upregulates PKCδ signal in HCECs. (**A**) HCECs were treated with vehicle control, PMA (1 μM), or rCAP37 (250 and 500 ng/mL) for 5 or 15 minutes as indicated. Cells were fixed in 4% paraformaldehyde for immunofluorescence analysis with anti-PKCδ and θ antibodies. PKCδ and PKCθ were visualized using AlexaFluor 488 goat anti-mouse secondary antibody. Nuclei are visualized with DAPI staining. Staining of PKCδ and PKCθ in HCECs was observed by confocal microscopy. Representative images are shown. *Scale bars*: 20 μm. (**B**) rCAP37 (500 ng/mL) was preincubated with anti-CAP37 monospecific, rabbit antiserum (0.002 μg/mL) for 30 minutes before treatment. HCECs were treated with vehicle control; PDGF-BB (20 ng/mL); or rCAP37 (500 ng/mL) for 15 minutes and processed as described in (**A**) above. *Scale bars*: 20 μm.

To determine if the marked increase in PKCδ staining seen in Figure 5 correlated to an increase in PKCδ protein level, total PKCδ was semiquantitated in CAP37-treated HCECs (Fig. 6A). An increase in PKCδ was seen in response to CAP37 treatment. A maximum response was obtained with 500 ng/mL of CAP37. These findings were corroborated using primary HCECs (Fig. 6A).

To examine whether CAP37 leads to phosphorylation of PKCδ, Western blot analysis of lysates from treated and nontreated HCECs was performed. Findings indicated in Figure 6B revealed a significant increase in the phosphorylation of PKCδ-Thr^{505} in response to treatment with 250 and 500 ng/mL of CAP37 for 5 minutes at 37°C when normalized to β-actin (Fig. 6B). A significant increase in phosphorylation was also seen in response to PMA (positive control). Because we previously showed an increase in total PKCδ expression level (Fig. 6A), we then normalized phosphorylated PKCδ-Thr^{505} to total PKCδ (Fig. 6C), and the results further confirm an increase in phosphorylation of PKCδ. These results indicate that CAP37 induces both PKCδ expression and the phosphorylation of PKCδ-Thr^{505}.

To measure the enzymatic activity of PKCδ, a kinase assay was carried out on CAP37-(250 ng/mL) treated and vehicle-treated HCECs after the immunoprecipitation of PKCδ, in presence of increasing amounts of substrate (CREBtide; Fig. 7). Kinase activity studies showed a time-dependent activation of PKCδ enzymatic activity (Fig. 7). There was a significant, 2-fold increase in PKCδ kinase activity in CAP37-treated cells when compared with vehicle-treated cells at 15 minutes. This result demonstrates that a net increase in total PKCδ enzymatic activity is mediated by CAP37 in HCECs and further supports the conclusion that this isoform is responsible for chemotaxis observed with these cells.

Discussion

Previous studies from our laboratory have demonstrated that CAP37 is a potent chemoattractant for host cells including corneal epithelial cells. However, the signaling mechanisms

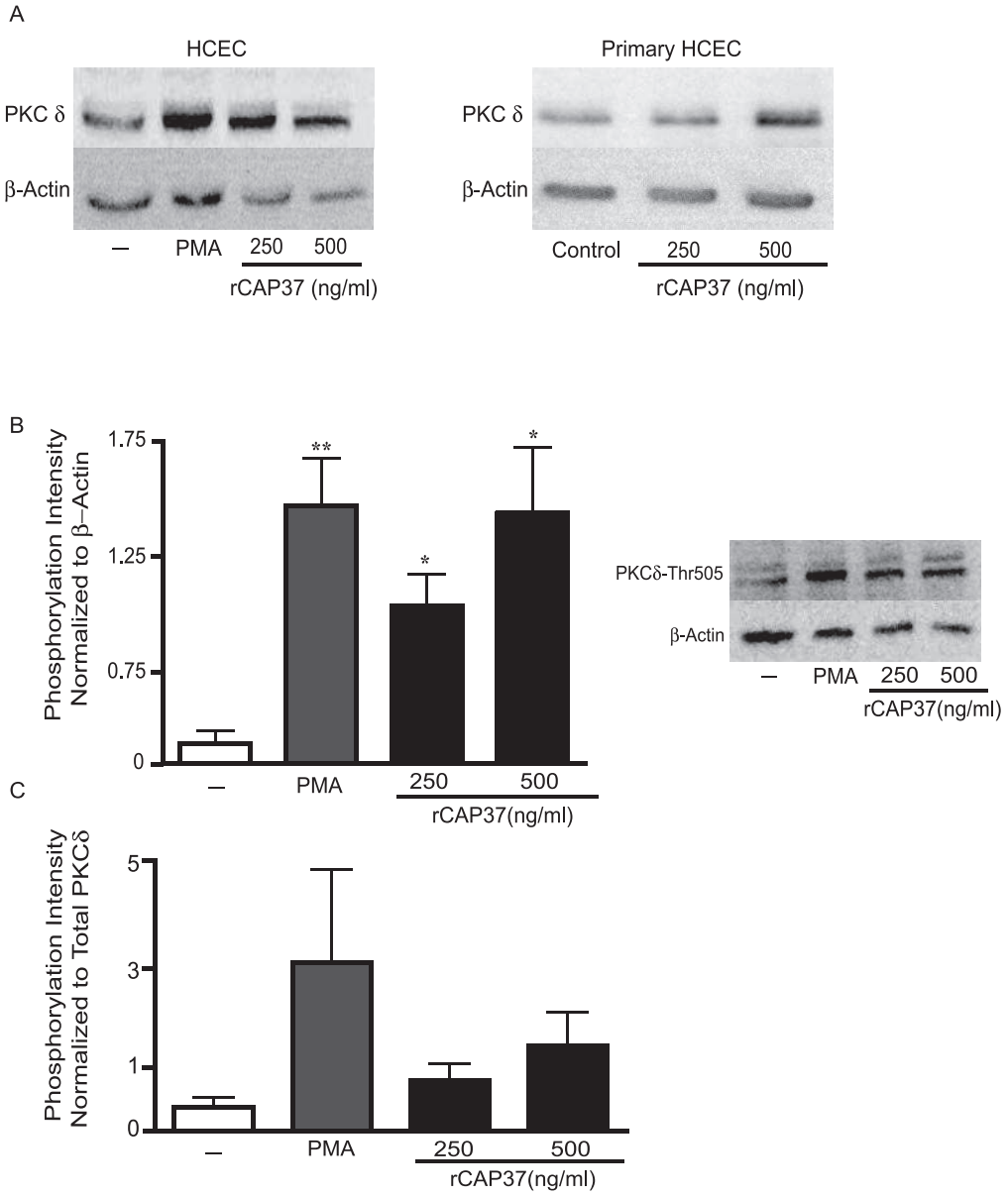

Figure 6. CAP37 leads to an increase in expression and phosphorylation of PKCδ. (**A**) HCECs were treated with rCAP37 (250 and 500 ng/mL) and PMA for 5 minutes and lysates (40 μg protein) were analyzed by Western blot for total PKCδ. Primary HCECs were treated with rCAP37 (250 and 500 ng/mL) for 5 minutes and lysates (4 μg) were analyzed for total PKCδ expression. β-actin loading controls are included for each blot. (**B**) Western blot analysis for PKCδ-Thr^{505} phosphorylation and β-actin following vehicle (–), PMA (1 μM), and CAP37 (250 and 500 ng/mL) treatment. A representative immunoblot is shown. The histogram shows phosphorylation signals normalized to β-actin and the mean of three independent experiments is shown ± SEM. *$P < 0.05$ by unpaired *t*-test. (**C**) Histogram showing the normalized PKCδ-Thr^{505} phosphorylation signals divided by the normalized PKCδ signal. The mean of three independent experiments is shown ± SEM.

activated by CAP37 to induce migration remained unclear. This study was undertaken to identify the signaling pathway employed by CAP37 in its mediation of corneal epithelial cell migration. Our findings demonstrate that CAP37 specifically activates the delta isoform of PKC.

During the process of chemotaxis, a chemoattractant such as CAP37 interacts with a receptor on the cell surface to activate signaling cascades resulting in modifications of the cytoskeleton leading to the orchestrated consecutive steps of protrusion, adhesion, traction, and retraction allowing migration along the gradient of the chemoattractant.[1,37] The complete inhibition of CAP37-mediated chemotaxis by PT (Fig. 1A) suggests that CAP37 induces chemotaxis through a GPCR. Numerous studies have demonstrated that PT specifically ADP-ribosylates G-protein alpha subunits belonging to the G_i family of heterotrimeric G-proteins coupled to GPCRs.[26,38] The ADP-ribosylation of the G_i protein by PT inactivates the G_i coupled-protein signaling pathway essential to chemotaxis.[26,38] This known mechanism of action by PT suggests that CAP37 mediates HCEC chemotaxis through activation of a GPCR and that a G_i-protein alpha subunit is involved.

Engagement of a GPCR commonly leads to the activation of PKA and PKC signaling pathways leading to MAPK activation.[33,34] To determine which specific pathway is involved in CAP37-mediated chemotaxis of HCECs, pharmacological inhibitors were used. The lack of inhibition of CAP37-mediated chemotaxis in response to highly effective PKA (H-89) and MAPK (JNK Inhibitor II and PD98059) pathway inhibitors

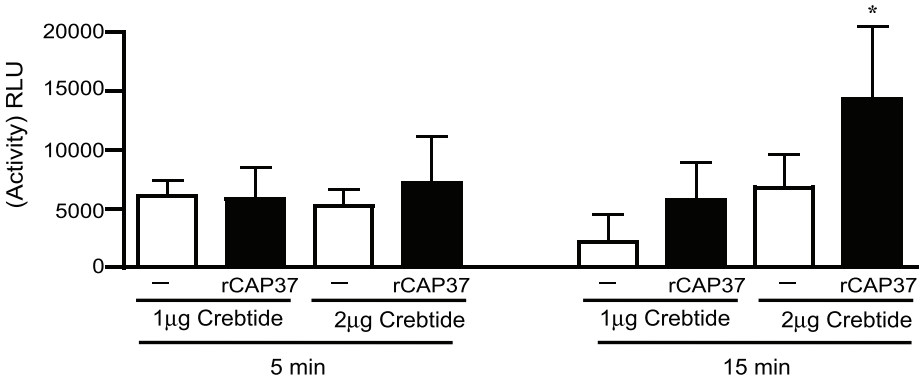

Figure 7. CAP37 activates PKCδ. HCECs were treated with a vehicle (–) or rCAP37 (250 and 500 ng/mL) for 5 and 15 minutes. Lysates were prepared from treated HCECs and immunoprecipitated with an anti-PKCδ antibody. The pulled-down enzyme was incubated for 1 hour at RT with 50 μM ATP and various concentrations of CREBtide substrate (0, 1, or 2 μg). Kinase activity of PKCδ is expressed as relative light units and measured using the kinase assay (Promega) as specified by the manufacturer. The mean of six independent experiments is shown ± SEM. $^*P < 0.05$ by Wilcoxon signed-rank test as compared with vehicle-treated controls.

suggests that PKA and MAPK pathways are not involved in CAP37-mediated chemotaxis. By contrast, the significant inhibition of CAP37-mediated chemotaxis by the highly specific PKC inhibitors calphostin c and Ro-31-8220 indicates a role for the PKC pathway (Fig. 1B).

Signaling through the PKC pathway involves the activation of specific PKC isoforms belonging to the classical, novel, or atypical family of PKCs. This study revealed that PKC isoforms α, δ, ε, θ, η, ζ, ι, and λ are expressed at detectable levels in HCECs, whereas the classical PKC isoforms β and γ are not (Fig. 2). PKC isoforms were depleted from HCECs through a prolonged treatment with the phorbol ester, PDBu. PDBu is a well-characterized reagent that mimics the effect of DAG. PDBu irreversibly binds and activates PKCs, which leads to their depletion.[16] Since phorbol esters mimic DAG, only the classical and novel PKCs are depleted in response to PDBu (Fig. 3A). Novel PKCη and atypical PKC isoforms ζ, ι, and λ are not activated by DAG and are not sensitive to PDBu depletion (Fig. 3A). Chemotaxis studies revealed that CAP37-mediated migration was completely inhibited after PDBu depletion (Fig. 3C). These studies suggest that PDBu sensitive PKC isoforms α, δ, ε, or θ are involved in mediating CAP37-dependent HCEC migration. Further chemotaxis studies involving the knockdown of PKCs α, δ, ε, or θ indicate that PKCδ and PKCθ are involved in CAP37-mediated HCEC chemotaxis. The complete inhibition of chemotaxis in response to CAP37 after the knockdown of either PKCδ or θ suggests that these two isoforms may control different mechanisms, both necessary for chemotaxis. PKCα and PKCε were not significantly involved in CAP37-mediated migration.

Our chemotaxis results support the involvement of both PKCδ and PKCθ. Thus, confocal microscopy was used to visualize PKCδ and PKCθ expression in HCEC in response to CAP37 treatment (Figs. 5A, 5B). While these studies revealed that PKCδ and PKCθ signals both responded to CAP37, there was a predominant increase in PKCδ staining that prompted further quantification of expression levels, phosphorylation, and activity of the enzyme. Subcellular fractionation studies (data not shown) indicated that there was a clear translocation of PKCδ from cytoplasm to membrane in response to CAP37. The translocation of PKCθ remained equivocal, prompting us to focus on PKCδ in this manuscript. The involvement of PKCθ in CAP37-mediated processes remains under investigation. Western blotting of CAP37-treated HCEC lysates revealed a rapid increase in total PKCδ by 5 minutes (Fig. 6A). Others have shown a similar rapid increase in PKCδ in skeletal muscle cells following insulin treatment due to an increase in transcription and translation.[39] We suggest that CAP37 could increase PKCδ expression through similar mechanisms. CAP37 signaling may lead to the activation of NF-κB, a potential transcription factor for PKCδ.[40,41] Support for this idea is based on studies that have shown that PT sensitive GPCR pathways can induce activation of NF-κB transcription through the Gβγ subunit.[38,42,43] Further studies are required to determine the mechanism of action through which this rapid increase in PKCδ expression occurs.

PKCδ is activated by the secondary messenger DAG that can lead to the association with the cell membrane followed by phosphorylation.[44] The PKCδ isoform is specifically regulated through serine, threonine, and tyrosine phosphorylation sites. PKCδ-Thr^{505} phosphorylation in CAP37-treated HCECs (Fig. 6A) is indicative of PKC activation, but does not directly demonstrate it. Studies in platelets have demonstrated that the binding of PKCδ by DAG results in PKCδ-Thr^{505} phosphorylation and translocation of PKCδ to the cell membrane.[45] Furthermore, studies show that phosphorylation of PKCδ-Thr^{505} is induced by the stimulation of GPCR agonists and leads to the accumulation of the secondary messenger DAG[14] and further supports the involvement of a GPCR. While the role of phosphorylation in PKC activation is not entirely understood, some studies suggest that the phosphorylation of PKCδ-Thr^{505} alters the activity of PKCδ toward certain substrates.[46] Since phosphorylation alone does not demonstrate the ability of CAP37 to directly activate PKCδ activity, a kinase activity assay was used to verify that CAP37 treatment directly results in PKCδ activation, further supporting the hypothesis that CAP37 mediates HCEC chemotaxis through the PKC pathway.

As the PKC signaling pathway continues to be understood, studies indicate a dynamic regulation of the PKC pathway and ability of PKCs, specifically PKCδ, to regulate cellular processes such as proliferation and chemotaxis,[47] and it has been implicated as a regulatory molecule in a number of diseases including cancer, diabetes, and Alzheimer disease.[47–49] Since chemotaxis is an essential process for proper wound healing, understanding the mechanism whereby CAP37 regulates cell migration is important in determining whether it plays a role in corneal wound healing. Taken together, this study indicates that CAP37, upon binding to a GPCR receptor, activates the PKC signaling cascade through the PKCδ isoform

Investigative Ophthalmology & Visual Science

leading to CAP37-directed HCEC chemotaxis. The specific GPCR through which CAP37 mediates signaling, the role of PKCθ, and events that occur downstream from PKC signaling will remain the focus of future studies.

Acknowledgments

The authors thank Jim Henthorn, Director, University of Oklahoma Health Sciences Center Flow Cytometry and Confocal Microscopy Laboratory, for his assistance with confocal microscopy and Ryan D. Webb and Sandra M. Carter for their assistance in performing the statistical analysis.

Supported by PHS Grants 5R01EY015534 (HAP), 5T32AI007633-08, and the Ford Fellowship Foundation (GLG).

Disclosure: **G.L. Griffith**, None; **R.A. Russell**, None; **A. Kasus-Jacobi**, None; **E. Thavathiru**, None; **M.L. Gonzalez**, None; **S. Logan**, None; **H.A. Pereira**, None

References

1. Kay RR, Langridge P, Traynor D, Hoeller O. Changing directions in the study of chemotaxis. *Nature Rev Mol Cell Biol*. 2008;9:455–463.
2. Amulic B, Cazalet C, Hayes GL, Metzler KD, Zychlinsky A. Neutrophil function: from mechanisms to disease. *Annu Rev Immunol*. 2012;30:459–489.
3. Pereira HA, Shafer WM, Pohl J, Martin LE, Spitznagel JK. CAP37, a human neutrophil-derived chemotactic factor with monocyte specific activity. *J Clin Invest*. 1990;85:1468–1476.
4. Pereira HA. CAP37, a neutrophil-derived multifunctional inflammatory mediator. *J Leukoc Biol*. 1995;57:805–812.
5. Pereira HA, Ruan X, Gonzalez ML, Tsyshevskaya-Hoover I, Chodosh J. Modulation of corneal epithelial cell functions by the neutrophil-derived inflammatory mediator CAP37. *Invest Ophthalmol Vis Sci*. 2004;45:4284–4292.
6. Lee TD, Gonzalez ML, Kumar P, Grammas P, Pereira HA. CAP37, a neutrophil-derived inflammatory mediator, augments leukocyte adhesion to endothelial monolayers. *Microvasc Res*. 2003;66:38–48.
7. Lee TD, Gonzalez ML, Kumar P, Chary-Reddy S, Grammas P, Pereira HA. CAP37, a novel inflammatory mediator: its expression in endothelial cells and localization to atherosclerotic lesions. *Am J Pathol*. 2002;160:841–848.
8. Ruan X, Chodosh J, Callegan MC, et al. Corneal expression of the inflammatory mediator CAP37. *Invest Ophthalmol Vis Sci*. 2002;43:1414–1421.
9. Pereira HA, Ruan X, Kumar P. Activation of microglia: a neuroinflammatory role for CAP37. *Glia*. 2003;41:64–72.
10. Morgan JG, Pereira HA, Sukiennicki T, Spitznagel JK, Larrick JW. Human neutrophil granule cationic protein CAP37 is a specific macrophage chemotaxin that shares homology with inflammatory proteinases. *Adv Exp Med Biol*. 1991;305:89–96.
11. Gonzalez ML, Ruan X, Kumar P, Grammas P, Pereira HA. Functional modulation of smooth muscle cells by the inflammatory mediator CAP37. *Microvasc Res*. 2004;67:168–181.
12. Imanishi J, Kamiyama K, Iguchi I, Kita M, Sotozono C, Kinoshita S. Growth factors: importance in wound healing and maintenance of transparency of the cornea. *Prog Retin Eye Res*. 2000;19:113–129.
13. Pereira HA, Moore P, Grammas P. CAP37, a neutrophil granule-derived protein stimulates protein kinase C activity in endothelial cells. *J Leukoc Biol*. 1996;60:415–422.
14. Steinberg SF. Structural basis of protein kinase C isoform function. *Physiol Rev*. 2008;88:1341–1378.
15. O'Connell MJ, Raleigh JM, Verkade HM, Nurse P. Chk1 is a wee1 kinase in the G2 DNA damage checkpoint inhibiting cdc2 by Y15 phosphorylation. *EMBO J*. 1997;16:545–554.
16. Dempsey EC, Newton AC, Mochly-Rosen D, et al. Protein kinase C isozymes and the regulation of diverse cell responses. *Am J Physiol Lung Cell Mol Physiol*. 2000;279:L429–438.
17. Suzuki K, Saito J, Yanai R, et al. Cell-matrix and cell-cell interactions during corneal epithelial wound healing. *Prog Retin Eye Res*. 2003;22:113–133.
18. Newton AC. Lipid activation of protein kinases. *J Lipid Res*. 2009;50:S266–S271.
19. Araki-Sasaki K, Ohashi Y, Sasabe T, et al. An SV40-immortalized human corneal epithelial cell line and its characterization. *Invest Ophthalmol Vis Sci*. 1995;36:614–621.
20. Li Y, Santos CM, Kumar A, et al. "Click" immobilization on alkylated silicon substrates: model for the study of surface bound antimicrobial peptides. *Chemistry*. 2011;17:2656–2665.
21. Rezaie AR, Esmon CT. The function of calcium in protein C activation by thrombin and the thrombin-thrombomodulin complex can be distinguished by mutational analysis of protein C derivatives. *J Biol Chem*. 1992;267:26104–26109.
22. Rezaie AR, Neuenschwander PF, Morrissey JH, Esmon CT. Analysis of the functions of the first epidermal growth factor-like domain of factor X. *J Biol Chem*. 1993;268:8176–8180.
23. Pereira HA. Assay systems for measurement of chemotactic activity. *Methods Mol Biol*. 1997;78:233–246.
24. Niemann MA, Bhown AS, Bennett JC, Volanakis JE. Amino acid sequence of human D of the alternative complement pathway. *Biochemistry*. 1984;23:2482–2486.
25. Tamura M, Nogimori K, Murai S, et al. Subunit structure of islet-activating protein, pertussis toxin, in conformity with the A-B model. *Biochemistry*. 1982;21:5516–5522.
26. Carbonetti NH. Pertussis toxin and adenylate cyclase toxin: key virulence factors of Bordetella pertussis and cell biology tools. *Future Microbiol*. 2010;5:455–469.
27. Piiper A, Gebhardt R, Kronenberger B, Giannini CD, Elez R, Zeuzem S. Pertussis toxin inhibits cholecystokinin- and epidermal growth factor-induced mitogen-activated protein kinase activation by disinhibition of the cAMP signaling pathway and inhibition of c-Raf-1. *Mol Pharmacol*. 2000;58:608–613.
28. Yang LJ, Baffy G, Rhee SG, Manning D, Hansen CA, Williamson JR. Pertussis toxin-sensitive Gi protein involvement in epidermal growth factor-induced activation of phospholipase C-gamma in rat hepatocytes. *J Biol Chem*. 1991;266:22451–22458.
29. Liang MN, Garrison JC. The epidermal growth factor receptor is coupled to a pertussis toxin-sensitive guanine nucleotide regulatory protein in rat hepatocytes. *J Biol Chem*. 1991;266:13342–13349.
30. Le Stunff H, Mikami A, Giussani P, et al. Role of sphingosine-1-phosphate phosphatase 1 in epidermal growth factor-induced chemotaxis. *J Biol Chem*. 2004;279:34290–34297.
31. Ramachandran R, Mihara K, Chung H, et al. Neutrophil elastase acts as a biased agonist for proteinase-activated receptor-2 (PAR2). *J Biol Chem*. 2011;286:24638–24648.
32. Sun R, Iribarren P, Zhang N, et al. Identification of neutrophil granule protein cathepsin G as a novel chemotactic agonist for the G protein-coupled formyl peptide receptor. *J Immunol*. 2004;173:428–436.
33. Vilardaga JP, Agnati LF, Fuxe K, Ciruela F. G-protein-coupled receptor heteromer dynamics. *J Cell Sci*. 2010;123:4215–4220.
34. Lappano R, Maggiolini M. G protein-coupled receptors: novel targets for drug discovery in cancer. *Nat Rev Drug Discov*. 2011;10:47–60.

Investigative Ophthalmology & Visual Science

35. Ronnstrand L, Heldin CH. Mechanisms of platelet-derived growth factor-induced chemotaxis. *Int J Cancer*. 2001;91:757–762.
36. Xu KP, Dartt DA, Yu FS. EGF-induced ERK phosphorylation independent of PKC isozymes in human corneal epithelial cells. *Invest Ophthalmol Vis Sci*. 2002;43:3673–3679.
37. Vorotnikov AV. Chemotaxis: movement, direction, control. *Biochemistry Biokhimiia*. 2011;76:1528–1555.
38. Sun L, Ye RD. Role of G protein-coupled receptors in inflammation. *Acta Pharmacol Sin*. 2012;33:342–350.
39. Horovitz-Fried M, Cooper DR, Patel NA, et al. Insulin rapidly upregulates protein kinase C delta gene expression in skeletal muscle. *Cell Signal*. 2006;18:183–193.
40. Kurkinen KM, Keinanen RA, Karhu R, Koistinaho J. Genomic structure and chromosomal localization of the rat protein kinase Cdelta-gene. *Gene*. 2000;242:115–123.
41. Suh KS, Tatunchak TT, Crutchley JM, Edwards LE, Marin KG, Yuspa SH. Genomic structure and promoter analysis of PKC-delta. *Genomics*. 2003;82:57–67.
42. Cowen DS, Molinoff PB, Manning DR. 5-hydroxytryptamine1A receptor-mediated increases in receptor expression and activation of nuclear factor-kappaB in transfected Chinese hamster ovary cells. *Mol Pharmacol*. 1997;52:221–226.
43. Yang M, Sang H, Rahman A, Wu D, Malik AB, Ye RD. G alpha 16 couples chemoattractant receptors to NF-kappa B activation. *J Immunol*. 2001;166:6885–6892.
44. Newton AC. Protein kinase C: structure, function, and regulation. *J Biol Chem*. 1995;270:28495–28498.
45. Murugappan S, Tuluc F, Dorsam RT, Shankar H, Kunapuli SP. Differential role of protein kinase C delta isoform in agonist-induced dense granule secretion in human platelets. *J Biol Chem*. 2004;279:2360–2367.
46. Liu Y, Belkina NV, Graham C, Shaw S. Independence of protein kinase C-delta activity from activation loop phosphorylation: structural basis and altered functions in cells. *J Biol Chem*. 2006;281:12102–12111.
47. Basu A, Pal D. Two faces of protein kinase Cdelta: the contrasting roles of PKCdelta in cell survival and cell death. *ScientificWorldJournal*. 2010;10:2272–2284.
48. Ciccocioppo F, Lanuti P, Marchisio M, et al. Expression and phosphorylation of protein kinase C isoforms in Abeta (1-42) activated T lymphocytes from Alzheimers disease. *Int J Immunopathol Pharmacol*. 2008;21:23–33.
49. Geraldes P, King GL. Activation of protein kinase C isoforms and its impact on diabetic complications. *Circ Res*. 2010;106:1319–1331.

Investigative Ophthalmology & Visual Science